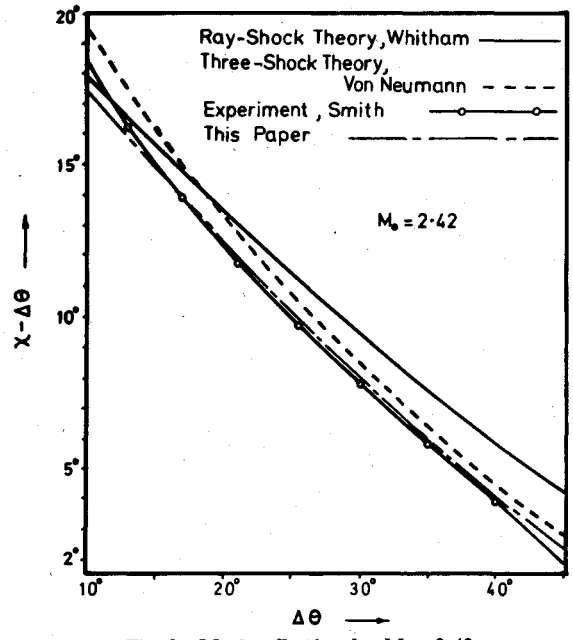

Fig. 3 Mach reflection for $M_0 = 2.42$.

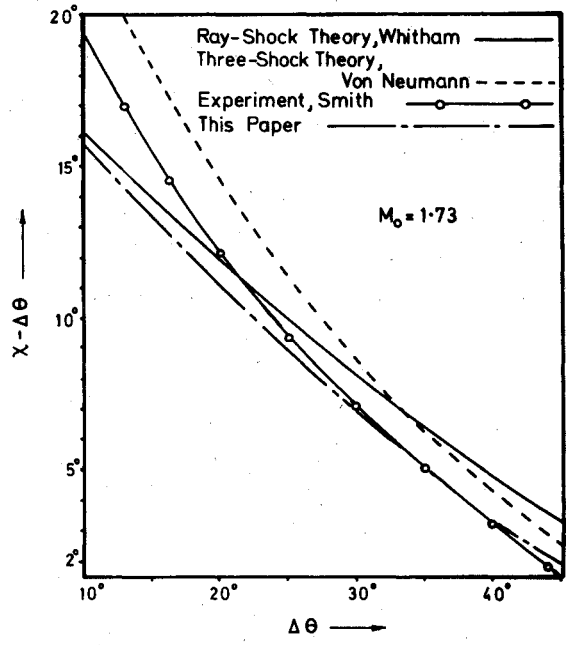

Fig. 4 Mach reflection for $M_0 = 1.73$.

For $\gamma = 1.4$

$$\eta = 0.546[1 - (M_0^2/M^2)] + \tfrac{1}{2}\ln A_0/A \qquad (19)$$

At glancing incidence, $M = M_0$ and $A = A_0$, making $\eta = 0$ and reducing Eq. (17) to Eq. (1).

Comparison of Theory and Experiment

Equation (17) has been used in combination with the normal ray-shock kinematic equations to obtain new results for the Mach reflection geometry. These are presented in Figs. 3 and 4 for incident shock Mach numbers 2.42 and 1.73. Comparisons are made in each case with the normal ray-shock theory, the three-shock theory, and experiment (Smith).[9] At the highest experimental Mach number, good agreement exists between the present method and Smith's experiments for the range of corner angles $14° < \Delta\theta < 40°$. At the lower corner angles the experimental curve deviates upwards, as would be expected from the observed appearance at low $\Delta\theta$ values of noticeable stem curvature. As $\Delta\theta$ approaches 45°, the curves again separate because the ray-shock theory continues to predict Mach reflection above values where regular reflection is known to occur.

As the incident Mach number is lowered, the range of agreement, although markedly improved over the unmodified ray-shock theory, and the three-shock theory, becomes smaller. This is because the stem curvature becomes more noticeable with reduced strength. At a shock strength of $M_0 = 1.73$ the range of good agreement has reduced to $30° < \Delta\theta < 40°$. Other comparisons at $M_0 = 2.10$ and 1.51 show very close agreement in the ranges $20° < \Delta\theta < 40°$ and $30° < \theta < 37°$, respectively.

It should be noted that correction terms have been evaluated using strong shock equations for the shock front. A more accurate value for η should be obtained by using the exact equations. However, in view of the accuracy of the results, this extra complexity does not seem necessary.

References

[1] Von Neumann, J., "Theory of Shock Waves," *Collected Works*, Vol. VI, Pergamon Press, N.Y., 1963, pp. 238-299.

[2] Whitham, G. B., "A New Approach to Problems of Shock Dynamics, Part 1, Two-Dimensional Problems," *Journal of Fluid Mechanics*, Vol. 2, March 1957, pp. 145-171.

[3] Chester, W., "The Quasi Cylindrical Shock Tube," *Philosophical Magazine*, Vol. 45, Dec. 1954, pp. 1293-1301.

[4] Chisnell, R. F., "The Motion of a Shock Wave in a Channel with Applications to Cylindrical and Spherical Shock Waves," *Journal of Fluid Mechanics*, Vol. 2, May 1957, pp. 286-298.

[5] Yousaf, M., "The Effect of Overtaking Disturbances on the Motion of Converging Shock Waves," *Journal of Fluid Mechanics*, Vol. 66, Nov. 1974, pp. 577-591.

[6] Whitham, G. B., "On the Propagation of Shock Waves through Regions of Non-Uniform Area or Flow," *Journal of Fluid Mechanics*, Vol. 4, Aug. 1958, pp. 337-360.

[7] Rosciszewski, J., "Calculations of the Motion of Non-Uniform Shock Waves," *Journal of Fluid Mechanics*, Vol. 8, July 1960, pp. 337-367.

[8] Oshima, K., Sugaya, K., Yamamoto, M., and Totoki, T., "Diffraction of a Plane Shock Wave around a Corner," Rept. No. 393, Jan. 1965, Institute of Space and Aeronautical Science, Univ. of Tokyo.

[9] Smith, L. G., "Photographic Investigation of the Reflection of Plane Shocks in Air," Rept. 6271, Nov. 1945, Office of Scientific Research and Development.

Motion of a Stretched Cable with Small Curvature Carrying and Accelerating Mass

M. J. Forrestal,* D. C. Bickel,† and M. J. Sagartz‡
Sandia Laboratories, Albuquerque, N. Mex.

ROCKET-POWERED trolleys traveling along an aerial cable are used to simulate aircraft flight for the evaluation of airborne equipment at Sandia Laboratories, Albuquerque. The 1465 m long, 35 mm diameter steel cable is suspended between two mountain peaks. A winch positions the cable to heights up to 220 m above the canyon floor by tensioning up to 490 kN. At this tension, maximum sag is 30

Received June 16, 1975. This work was supported by the U.S. Energy Research and Development Administration.

Index category: Structural Dynamic Analysis.

*Division Supervisor, Shock Simulation Department. Associate Fellow AIAA.

†Division Supervisor, Shock Simulation Department.

‡Staff Member, Shock Simulation Department.

m below a straight line between the ends of the cable. Trolleys are propelled at nearly constant acceleration up to velocities of 300 m/sec.

To estimate the cable motion, formulas are derived for the response of a slightly curved, semi-infinite cable carrying a mass which moves at constant acceleration. The analysis assumes the cable is loaded by forces corresponding to the weight of the mass and the normal acceleration of the mass moving along the static equilibrium configuration of the cable. Thus, the analysis neglects the interaction of cable and mass motion; e.g., see Refs. 1, 2. In a previous publication,[3] the authors considered a straight cable loaded by a traveling force moving at constant acceleration; this paper considers the additional force corresponding to normal acceleration and presents a comparison of measured and predicted cable deflection.

Analysis

In this section it is shown that the radius of curvature for the cable is nearly constant and formulas for cable motion produced by an accelerating mass moving along a constant curvature are presented. From Ref. 4, curvature can be written as

$$K=(\rho g/T)\cos\theta \tag{1}$$

where T is the cable tension at the end support, ρ is mass per unit length, g is the acceleration due to gravity, and θ is the cable slope measured from the horizontal. For small angle θ

$$K=\frac{\rho g}{T}\left[1-\tfrac{1}{2}\left(\frac{\rho g s}{T}\right)+\ldots\right] \tag{2}$$

in which s is measured along the cable from the point of maximum sag where $\theta=0$. For the application in this Note, the second term in the above bracket is less than 1% and curvature is taken as the constant

$$K=(1/R)=(\rho g/T) \tag{3}$$

where R is the radius of curvature.

For the previously stated assumptions, the loading consists of two parts; the force due to the weight of the mass given by

$$p_1(x,t)=Mg\cdot\delta(x-at^2/2) \tag{4}$$

and the reaction from the normal acceleration given by

$$p_2(x,t)=\frac{MV^2}{R}\cdot\delta(x-at^2/2)=\frac{Ma^2t^2}{R}\cdot\delta(x-at^2/2) \tag{5}$$

where M is the mass, a is the constant acceleration, V is the velocity of the traveling mass, x is the coordinate along the cable measured from the pinned end, δ is the Dirac delta function, and t is time.

The solution for the loading given by Eq. (4) is presented in Ref. 3 and the solution for the loading given by Eq. (5) is presented in this Note. Since the problem is linear, the cable motions may be written as

$$y(x,t)=y_1(x,t)+y_2(x,t) \tag{6}$$

where y_1 and y_2 represent vertical displacements corresponding to the loads given by Eqs. (4 and 5), respectively. The equation of motion for y_2 is

$$\rho\frac{\partial^2 y_2}{\partial t^2}-T\frac{\partial^2 y_2}{\partial x^2}=\frac{Ma^2t^2}{R}\cdot\delta(x-at^2/2) \tag{7}$$

with the boundary condition $y_2(0,t)=0$ and quiescent initial conditions. Using the mathematical solution techniques

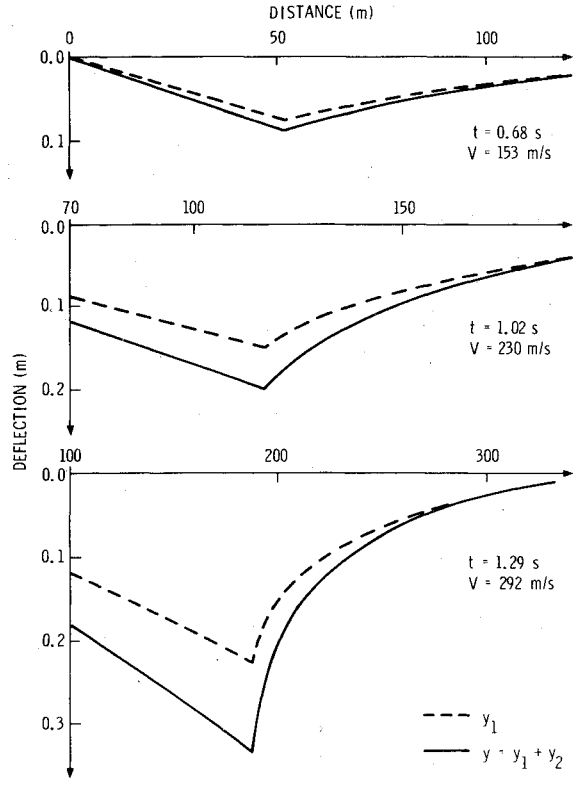

Fig. 1 Cable deflection profiles for $M=100$ kg, $T=490$ kN, $c=307$ m/sec, and $a=226$ m/sec^2.

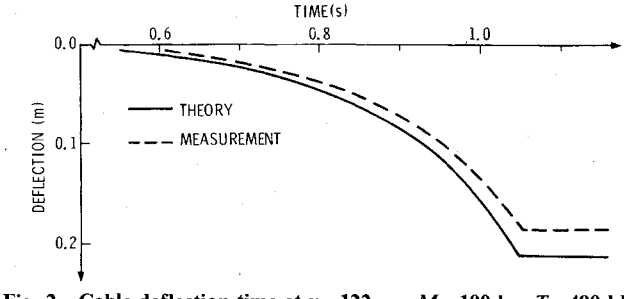

Fig. 2 Cable deflection-time at $x=122$, m, $M=100$ kg, $T=490$ kN, $c=307$ m/sec, and $a=226$ m/sec^2.

outlined in Ref. 3, the cable deflection is given by

$$y_2(x,t)=\frac{Mg(2a)^{1/2}}{2cT}\int_0^\infty \alpha^{1/2}d\alpha\left\{H\left[t-\left(\frac{2\alpha}{a}\right)^{1/2}-\frac{|x-\alpha|}{c}\right]-H\left[t-\left(\frac{2\alpha}{a}\right)^{1/2}-\frac{(x+\alpha)}{c}\right]\right\} \tag{8}$$

where $c^2=T/\rho$ and H is the Heaviside unit function. The term $\alpha^{1/2}$ integrates to give $2(\alpha)^{3/2}/3$ and the Heaviside functions determine the limits of integration.

The mass is moving at constant acceleration a, has velocity V, and location $x=at^2/2$. For the velocity V less than the propagation speed of cable disturbances, $V<c$, the response is

$$y_1(x,t)=0,\quad ct<x \tag{9a}$$

$$y_1(x,t)=Y(2D-B-C),\quad at^2/2<x<ct \tag{9b}$$

$$y_1(x,t)=Y(A-B),\quad 0<x<at^2/2 \tag{9c}$$

and

$$y_2(x,t)=0,\quad ct<x \tag{10a}$$

$$y_2(x,t) = Z[(D-C)^3 + (D-B)^3],\ at^2/2 < x < ct \quad (10b)$$

$$y_2(x,t) = Z[(D-B)^3 - (D-A)^3],\ 0 < x < at^2/2 \quad (10c)$$

in which

$$A(x,t) = (c^2/2a + ct + x)^{1/2}, B(x,t) = (c^2/2a + ct - x)^{1/2}$$

$$C(x,t) = (c^2/2a - ct + x)^{1/2}, D = (c^2/2a)^{1/2}$$

$$Y = Mg/[(2a)^{1/2}\rho c], Z = Mg(2a)^{1/2}/3cT \quad (11)$$

The kink angle under the mass at $x = at^2/2$ is obtained by differentiating the deflection formulas and calculating the slope differences. For the loading terms given by Eqs. (4 and 5), the kink angle Δ is

$$\Delta = \frac{Mg}{T}\left[\frac{1+(V/c)^2}{1-(V/c)^2}\right] \quad (12)$$

For the special case when $V = c$ and at the mass location

$$y_1 = 0.293\ Mg/\rho a,\ y_2 = 0.155\ Mg/\rho a,\ y = 0.448\ Mg/\rho a \quad (13)$$

Numerical Results and Comparison with a Test

Deflection profiles of y_1 and y are shown in Fig. 1 for $M = 100$ kg, $T = 490$ kN, $c = 307$ m/sec, $a = 226$ m/sec^2, at $t = 0.68$, 1.02 ane 1.29 sec. At these times the mass positions are $x = 52$, 118, and 188 m. As shown in Fig. 1, maximum deflection is at the mass location.

To determine the adequacy of the simplified mathematical model used in the analyses, the cable deflection at a known position was monitored with a framing camera. A comparison of measured and predicted deflections at $x = 122$ m is shown in Fig. 2. These data indicated that the predictions of cable motion are reasonably accurate.

References

[1] Fryba, L., *Vibration of Solids and Structures Under Moving Loads*, Noordholt International Publishing, Groningen, The Netherlands, 1972, pp. 44, 45.

[2] Lee, E. H., "On a Paradox in Beam Vibration Theory," *Quarterly of Applied Mathematics*, Vol. X, No. 2, Oct. 1952, pp. 290-292.

[3] Sagartz, M. J. and Forrestal, M. J., "Motion of a Stretched String Loaded by an Accelerating Force," *Journal of Applied Mechanics*, Vol. 42, Ser. E, No. 2, June 1975, pp. 505-506.

[4] Beer, F. P. and Johnston, E. R., *Mechanics for Engineers-Statics and Dynamics*, McGraw-Hill, San Francisco, Calif., 1962, pp. 253-254.

Effect of the Mass Center Shift for Force-Free Flexible Spacecraft

Leonard Meirovitch* and Jer-Nang Juang†
Virginia Polytechnic Institute and State University, Blacksburg, Va.

Introduction

As spacecraft increase in size, the weight problem is becoming progressively critical. One way of reducing the weight is to make the structural members as light as possible. But reduced structural weight generally implies reduced stiffness, so that the flexibility becomes an important factor in the spacecraft dynamic characteristics. Indeed, flimsy elastic members undergo large elastic deformations which can have a significant effect on the spacecraft stability and control.

In describing the motion of a spinning spacecraft, it is often convenient to refer the motion to a system of axes with the origin at the spacecraft mass center C. For flexible spacecraft the mass center C generally shifts relative to the nominal undeformed position, so that the system kinetic energy contains terms involving the shifting of C.[1] Quite often these terms complicate the stability analysis appreciably. It is shown in Ref. 2, however, that for a force-free flexible spacecraft of a particular configuration the stability criteria are not affected adversely by ignoring the shifting of C. The question arises naturally as to whether this is true in general. It is the purpose of this paper to address this question and to generalize the results of Ref. 2. Indeed, the paper proves that for the general class of force-free single-spin flexible spacecraft it is possible to ignore the shifting of the mass center relative to the nominal undeformed state without affecting the stability criteria in any significant way. The errors in the stability criteria so derived not only tend to be very small, but they are also on the safe side because such criteria are conservative compared to those obtained by including the shifting of C. The simplification in the stability analysis achieved by ignoring the shifting of C fully justifies the relatively small loss in accuracy.

Stability Analysis

Consider a force-free single-spin flexible spacecraft. Assuming that the orbital motion is known (and can be ignored), it is shown[1] that the system kinetic energy for motion relative to C can be written in the form

$$T = \tfrac{1}{2}\omega^T J\omega + \boldsymbol{K}^T\omega + \tfrac{1}{2}\int_m \dot{\boldsymbol{u}}_c'^T\dot{\boldsymbol{u}}_c' dm \quad (1)$$

where ω is the body angular velocity, J is inertia matrix in deformed state, $\boldsymbol{K}$ is the vector representing the angular momentum due to elastic velocities alone, and $\dot{\boldsymbol{u}}_c'$ is the vector of these elastic velocities measured relative to a set of body axes with the origin at C. For a force-free system the potential energy V_{EL} is due entirely to elastic deformations. Its expression is not affected by the shifting of the mass center. Taking into account the angular momentum integral, we conclude from Ref. 1 that the system is asymptotically stable if the functional

$$\kappa = T_0 + V_{EL} \quad (2)$$

is positive definite, where

$$T_0 = \tfrac{1}{2}\beta^T J^{-1}\beta \quad (3)$$

in which β is the conserved angular momentum vector.

The term T_0 involves the shifting x_c, y_c, z_c of the mass center. Because x_c, y_c, and z_c involve integrals of the elastic deformations, they do not represent additional generalized coordinates. Their presence in T_0, however, complicates the stability analysis appreciably, so that an examination of their role in the analysis is of vital interest. To this end, let us observe that J can be written in the form

$$J = J_u - J_c \quad (4)$$

where J_u is the inertia matrix obtained by ignoring x_c, y_c, and z_c and

$$J_c = m\begin{bmatrix} y_c^2+z_c^2 & -x_cy_c & -x_cz_c \\ -x_cy_c & x_c^2+z_c^2 & -y_cz_c \\ -x_cz_c & -y_cz_c & x_c^2+y_c^2 \end{bmatrix} \quad (5)$$

Received June 19, 1975. This investigation was supported by the NASA Research Grant NGR 47-004-126 sponsored by ESRO through the Stabilization and Control Branch, Goddard Space Flight Center.

Index categories: Spacecraft Attitude Dynamics and Control; Structural Dynamic Analysis.

*Professor, Department of Engineering Science and Mechanics. Associate Fellow AIAA.

†Postdoctoral Research Assistant, Department of Engineering Science and Mechanics. Presently Member of the Technical Staff, Computer Sciences Corporation, Attitude Determination Section, Silver Spring, Maryland.